One-dimensional model of a pulsed plasma thruster

T. R. Nada
tareknada@gmail.com
Emirates Aviation College
Dubai, UAE

ABSTRACT

This paper presents a modified one dimensional model for the pulsed plasma thruster. The model takes into account the impact of thruster geometry and capacitor initial energy on plasma inductance and resistance, as well as the ablated mass per pulse. These three factors have significant impact on the performance of the thruster and have not been considered concurrently before. The model is verified by comparing the estimated specific impulse, impulse bit and thrust-to-power ratio with experimental measurements for space qualified thrusters. The maximum error is estimated to be about 8% when using the modified model, while the conventional snowplow model produces error up to about 70%. The modified model is then employed to generate design charts that would help in selecting the proper combination of thruster geometry and energy level in the preliminary design phase of a pulsed plasma thruster for different space missions.

Paper No. 3844. Manuscript received 16 July 2012, revised version received 11 December 2012, accepted 18 March 2013.

https://doi.org/10.1017/S0001924000008599 Published online by Cambridge University Press

NOMENCLATURE

B magnetic field strength (Tesla)
C capacitance (Farad)
d width (m), see Fig. 1
E energy (J)
F thrust force (N)
h thrust force (N)
Ibit impulse bit (N.s)
Isp specific impulse (s)
J current (A)
L inductance (H)
L rate of change of inductance with distance (H/m)
M Mass (kg)
n_e electron density (m^{-3})
Q charge (Coulomb)
R resistance (Ω)
T time (s)
T_e electron temperature
V voltage (V)
x channel length (m)
η efficiency (%)
μ_o vacuum magnetic permeability ($8{\cdot}885 \times 10^{-12}$A.s/V.m)
τ characteristic pulse time (s)
ρ density (kg/m^3)

Subscripts

c capacitor
o initial
p plasma

Abbreviations

AR Aspect Ratio of thruster, h/d, see Fig. 1
LCR Inductance-Capacitance-Resistance
PPT Pulsed Plasma Thruster
PPU Power Processing Unit

1.0 INTRODUCTION

Of all the various electric thruster concepts, the pulsed plasma thruster (PPT) was the first to achieve acceptance for application on space missions because of its system simplicity and moderate to high specific impulse[1]. The robustness, short development time, and low cost of the PPT allowed its selection for space-flight applications in the 1960s, despite its low efficiency[1].

The model of pulsed plasma thruster must contain two main pieces; the first is the circuit analysis and model, while the second is the plasma dynamic model. In the first model, the basic equations are written for the LCR-circuit considering the plasma sheet as an element that

https://doi.org/10.1017/S0001924000008599 Published online by Cambridge University Press

completes this circuit. Simple assumptions are made to solve these equations[2]. The snowplow model takes into account multi ablated material while neglecting compressibility effect. For preliminary design and optimisation of thruster geometry, the sophisticated models such as multi-fluid and gas-kinetic models are not necessary, and the snowplow model with circuit analysis will be enough[3,4].

However, authors who employed the snowplow model did not consider the influences of geometry and capacitor energy in determining plasma resistance and inductance. Moreover, the ablated mass per pulse was presumed constant at some average value[4]. These three factors have significant impact on the performance of the thruster, and they have not been considered concurrently before. Thus, the snowplow model has three weak points; estimation of plasma resistance as function of thruster geometry and capacitor energy, the variation of inductance as the plasma travels between electrodes, and the estimation of ablated mass per pulse as function of propellant sublimation area and initial energy in the capacitor. According to the author's knowledge, the above three factors have not been considered simultaneously in any analytical model that can be employed in optimising the performance of thruster in the preliminary design phase.

In the preliminary design phase, when the first hardware prototype has not been built yet, it is difficult to guess the plasma resistance and the ablated mass per pulse. This is particularly true if the new design is far from existing ones in terms of geometry and/or energy level. Also, using constant values for plasma resistance and ablated mass per pulse would result in significant deviation in the estimated performance parameters, if a wide range of geometry and/or electrical parameters are to be investigated. Thus, it is required to build a robust, yet simple, one-dimensional model to investigate accurately wide range of geometry and energy to optimise the performance of the thruster for given mission.

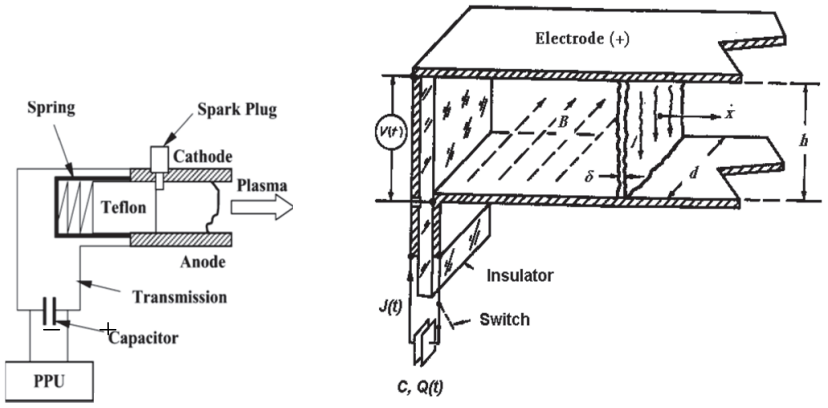
This paper presents a modified one dimensional snowplow model for the pulsed plasma thruster. The model takes into account the variations of plasma inductance and resistance as well as ablated mass per pulse with thruster geometry and capacitor initial energy. The model is verified by comparing the estimated values of specific impulse, impulse bit, and thrust-to-power ratio with experimental values for space qualified thrusters. The model is then employed to generate design charts that would help in selecting the proper combination of thruster geometry and capacitor energy in the preliminary design phase of a pulsed plasma thruster for different space missions.

2.0 MODIFIED SNOWPLOW MODEL

Figure 1 shows a schematic diagram and definition of geometry of PPT in its traditional, breech-fed, rectangular form. The thruster is driven by an LCR pulse circuit. In this arrangement, a solid propellant bar of Teflon® fills the gap between two electrodes connected to a charged capacitor. A spark igniter, which is mounted on the cathode, provides a small amount of initial plasma triggering an electrical discharge across the exposed surface of the Teflon. Heat transfer from this discharge causes evaporation of propellant material, which is then accelerated by electromagnetic and pressure forces. As the propellant evaporates with each discharge, a simple spring mechanism advances the propellant bar axially into the thrust chamber, eliminating the need for a propellant tank and feed-regulation system.

The snowplow model represents the simplest analytical model, which incorporates the sweeping feature and considers the current zone driven by its own magnetic field as an impermeable completely absorbing surface propagating into the ambient gas. The mass overtaken by this

https://doi.org/10.1017/S0001924000008599 Published online by Cambridge University Press



(a) Schematic drawing (b) Definition of geometrical parameters[2]

Figure 1. Pulsed plasma thruster.

advancing surface is assumed to be accumulated and subsequently to travel along the thruster; hence the name snowplow[2]. The circuit equation, Kirchhoff's law, can be written with the capacitor voltage included in the form

$$\frac{\mathrm{d}}{\mathrm{d}t}\left[J\left(L_o + L_1 x\right)\right] + JR + \frac{Q}{C} = \left(L_o + L_1 x\right)\dot{J} + JL_1\dot{x} + JR - V_o + \frac{1}{C}\int_0^t J\mathrm{d}t = 0 \quad \ldots (1)$$

The statement of Newton's law must contain an inertial term to allow for the rate of mass accumulation:

$$m\ddot{x} + \dot{m}\dot{x} = 0 \cdot 5L_1 J^2 \quad \ldots (2)$$

The current sheet, when initially formed, is assumed to embody a certain small but finite mass. After inception, the current sheet accumulates mass at a rate determined by the sheet velocity, the channel dimensions and the ambient mass density distribution. The density will be presumed uniform at the beginning:

$$m(x) = m_o + h\mathrm{d}\int_0^{t(x)} \rho(x)\dot{x}\mathrm{d}t = m_o + h\mathrm{d}\rho x \quad \ldots (3)$$

The dynamic equation may be written as:

$$(m_o + h\mathrm{d}\rho x)\ddot{x} + h\mathrm{d}\rho\dot{x}^2 = 0 \cdot 5L_1 J^2 \quad \ldots (4)$$

Equations (1) and (4) are simultaneous equations, in $J(t)$ and $x(t)$, in terms of the parameters m_o, L_o, L_1, V_o, C and total resistance. The total resistance equals to the sum of plasma and capacitor resistances. If total resistance is presumed constant throughout the dynamic process, these equations may be written in non-dimensional form to generalise numerical solutions as follow[2]:

$$x^* = \frac{L_1}{L_o}x \quad \ldots (5)$$

https://doi.org/10.1017/S0001924000008599 Published online by Cambridge University Press

$$t^* = \frac{1}{\sqrt{L_o C}} t \quad \ldots (6)$$

$$J^* = \frac{1}{V_o}\sqrt{\frac{L_o}{C}} J \quad \ldots (7)$$

The dynamic and circuit equations then take the forms:

$$(m^* + x^*)\ddot{x}^* + (\dot{x}^*)^2 = \alpha (J^*)^2 \quad \ldots (8)$$

$$(1 + x^*)\dot{J}^* + J^* \dot{x}^* + \beta J^* = 1 - \int_0^{t^*} J^* \mathrm{d}t^* \quad \ldots (9)$$

Where:

$$\alpha = \frac{C^2 V_o^2 L_1^2}{2\mu L_o} \quad \ldots (10)$$

$$\mu = hd\rho \frac{L_o}{L_1} \quad \ldots (11)$$

$$\beta = R\sqrt{\frac{C}{L_o}} \quad \ldots (12)$$

$$m^* = \frac{m_o}{\mu} \quad \ldots (13)$$

Regardless of the difficulty of its assumptions, the snowplow model is quite successful in predicting current sheet trajectories for a variety of pulsed plasma accelerators over a broad range of operation[4]. The solution of Equations 8 and 9 gives current and plasma travelling distance with time. A system of first order nonlinear ordinary differential equations is constructed by substitution. This system is solved in the time domain to give current and plasma travelling distance. Differentiation the displacement gives velocity and the differentiated voltage is nearly *J/C*, except for small corrections from R_C and L_C, that is[3]:

$$-C\frac{\mathrm{d}V}{\mathrm{d}t} = J + R_C C\frac{\mathrm{d}J}{\mathrm{d}t} + L_C C\frac{\mathrm{d}^2 J}{\mathrm{d}t^2} \quad \ldots (14)$$

Because the inductance $L_C << L$ and the capacitor resistance $R_C << R$, the last two terms may be neglected and the voltage will be simply the integration of current divided by the capacitance that is:

$$V(t_1) \approx V_O - \frac{1}{C}\int_0^{t_1} J(t)\cdot \mathrm{d}t \quad \ldots (15)$$

The Lorenz force is calculated from:

$$F(t) = \frac{\mu_o h \cdot J^2(t)}{2d} \quad \ldots (16)$$

https://doi.org/10.1017/S0001924000008599 Published online by Cambridge University Press

From this thrust variation with time, the impulse bit is calculated via:

$$I_{bit} = \int F(t) \cdot \mathrm{d}t = \mu_O \frac{h}{2d} \int J^2 \cdot \mathrm{d}t \qquad \ldots (17)$$

Finally, the thruster efficiency is evaluated from:

$$\eta = \frac{I_{bit}^2}{2m_O E_O} \qquad \ldots (18)$$

The above model has three weak points; estimation of plasma resistance as function of thruster geometry and capacitor energy, the variation of inductance as the plasma travels between electrodes and the estimation of ablated mass per pulse as function of propellant sublimation area and initial energy level in the capacitor. These three parameters have significant impacts on the evaluation of the overall performance of the thruster. Burton and *et al*[5] proposed to represent plasma inductance as a linear function with x:

$$L = L_o + L_1 x \qquad \ldots (19)$$

A model for L_O and L_1 is given as:

$$L_O = 0 \cdot 88d - 0 \cdot 4h \qquad [\mu\mathrm{H}] \qquad \ldots (20)$$

$$L_1 = 0 \cdot 6 + 0 \cdot 4 \mathrm{Log} \frac{h}{d} \qquad [\mu\mathrm{H}] \qquad \ldots (21)$$

The plasma resistance has significant influence on the developed current and hence plasma velocity, which determines specific impulse and thrust. Previous 1D models have utilised a constant value of resistance that was either experimentally measured or that yielded a best-fit with current and voltage waveforms[1]. However, Laperriere[6] proposed a non-linear model that relates plasma resistance to plasma temperature and thruster geometry:

$$R_P = 8 \cdot 08 \frac{h}{d T_e^{0 \cdot 75}} \sqrt{\frac{\mu_o \ln \left[1 \cdot 24 \times 10^7 \left(\frac{T_e^3}{n_e} \right)^{0 \cdot 5} \right]}{\tau}} \qquad \ldots (22)$$

The characteristic pulse time, τ, is equal to a quarter of the PPT ringing period. The thruster ringing period is the reciprocal of the frequency. According to the above model, the plasma resistance increases with the reduction of this ringing period. Electron temperature and density are mainly functions of energy. Laperriere[6] has employed the above model to estimate plasma resistance. However, he assumed constant electron temperature and density at some average values. On the other hand, Eckman[7] performed electron temperature and density measurements in the plume of a PPT at different energy levels. Figure 2 shows the average values of electron temperature and density at different energy levels as concluded from reference[7]. Moreover, the effect of thruster geometry is apparent in the plasma resistance model and this will help in optimising the thruster performance for different geometries and energies. Figure 3 shows the variation of plasma resistance with electron temperature at different aspect ratios assuming the electron density is $1 \times 10^{21} \mathrm{m}^{-3}$.

The only way to know the ablated mass per pulse is to measure the mass of the propellant bar before and after large number of pulses, and estimate the average mass per pulse. Till date,

https://doi.org/10.1017/S0001924000008599 Published online by Cambridge University Press

there is no accurate analytical model to predict the ablated mass per pulse. However, appropriate number of measurements is published for different energy levels and for different propellant sublimation area. Semi-empirical correlation is derived by curve fitting the available experimental data for thrusters actually employed on satellites, flight-qualified or laboratory-tested. A database for the measured ablated mass per pulse, for nine different thrusters that have different capacitor energy and/or propellant sublimation area, has been built from different references. The measured values for LES-6, NOVA, China Lab, LES-8/9, and Japan Lab thrusters have been obtained from Ref. (1). Also, measured values for TMIT-5, and TMIT-6a have been collected from Refs 8. Finally, measured values for SMS and SIMP-LEX thrusters have been obtained from Refs 9 and 10, respectively.

It is known that the ablated mass increases with the increase in energy and/or increase in propellant sublimation area. Thus, the ablated mass per unit area is estimated and plotted against the capacitor energy. Figure 4 shows the estimated ablated mass per unit area, in ($\mu g/cm^2$), against energy, in (J). Also, the best exponential curve fitting is shown in the same Fig. The exponential function that describes this curve is:

$$\frac{\Delta m}{A_P} = 2 \cdot 75 e^{E_O/38} \qquad \ldots (23)$$

The maximum error for this curve fitting is 18% and the variance is 0·4. This error between the measured mass per unit area and the estimated value using the exponential curve might look large. However, employing this exponential function gives a good approximation for ablated mass per pulse for any sublimation area in the range from 0·5 to 25cm^2 and any initial capacitor energy in the range from 1·7 to 70J. Therefore, it is expected to help in optimising the thruster performance for different thruster geometry and electrical parameters. Ignoring the variation of ablated mass per pulse with energy and sublimation area reduces the credibility of the model, especially if wide range of energy and/or propellant sublimation area is to be investigated.

3.0 MODEL VERIFICATIONS

Results of the model are compared with data of three space qualified pulsed plasma thrusters. Table 1 summarises the geometrical and operational parameters of LES-6, LES8/9, and the Primex thrusters. The geometrical parameters and measured performance are taken from Refs 1 and 11. The

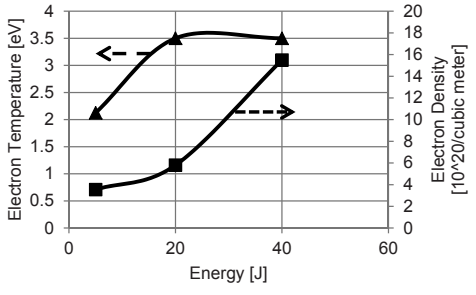


Figure 2. Electron density and temperature at different energies for d = 2·5cm and h = 3·8cm, concluded from Ref. 7.

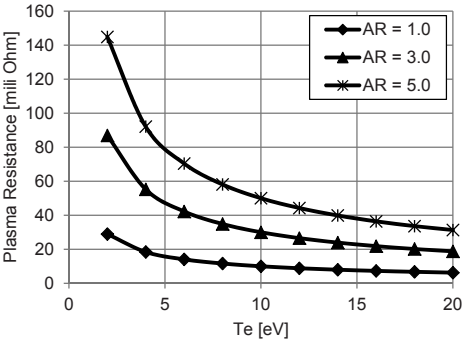


Figure 3. Plasma resistance at different electron temperature for different aspect ratios, at T_e = 1 × 10^{21}m^{-3} and τ = 0·2μs.

https://doi.org/10.1017/S0001924000008599 Published online by Cambridge University Press

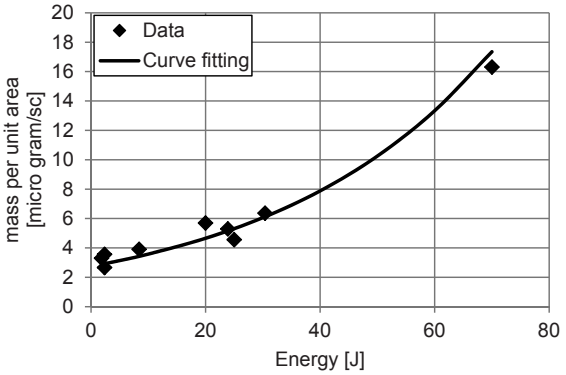


Figure 4. Ablated mass per pulse as function of energy.

investigated thrusters have; capacitor energy that spans from 1·85 to 43J, capacitance that varies from 2 to 33μF, and sublimation area ranges from 2·69 up to 24·8cm^2. Moreover, the produced specific impulse ranges from 300 to 1·121s, and the corresponding impulse bit ranges from 26 to 737μN.s.

Table 1
Geometrical and operational parameters of for LES-6, LES-8/9, and Primex thrusters

Thruster	E_o [J]	A_p [cm^2]	C [μF]
LES-6[1]	1·85	2·69	2
LES-8/9[1]	20	6·25	17
Primex[11]	43	24·8	33

Table 2 shows a comparison between measured and estimated performance parameters using the modified snowplow model. The estimated values for specific impulse, impulse bit, and thrust-to-power ratio agree well with the measurements with maximum error of about 8%. It is clear that the estimated error for Primex thruster is the largest error among the investigated thrusters for all performance parameters. For instant, the proposed model gives 8·1% error in the specific impulse for Primex thruster compared to 1·3% for LES-6 thruster and 0·3% for LES 8/9 thruster. Similarly, the model produces 7·9% error in the impulse bit for the Primex thruster compared to 2·7% and 4·4% for LES 6 and LES 8/9 thrusters, respectively. Also, it shows 6.3% error in the thrust to power ratio for Primex thruster compared to 2·1% and 4·2% for LES 6 and LES 8/9 thrusters, respectively. However, the estimated errors in all performance parameters for this thruster are still within an acceptable range for the preliminary design and system optimisation tasks.

For comparison and to prove the strength and robustness of the modified model, Table 3 shows a comparison between measured and estimated performance parameters using the original snowplow model. The snowplow model uses one average value for the ablated mass per pulse, and one average value for the plasma resistance for the three thrusters. The minimum error is 24%, while the maximum error is above 70%. It is apparent that, if the ablated mass per pulse and the plasma resistance are kept constant, the model fails to predict the correct performance parameters for wide variation in geometry and/or electrical parameters.

https://doi.org/10.1017/S0001924000008599 Published online by Cambridge University Press

Table 2
Measured and estimated parameters using the modified snowplow model

Thruster	Specific Impulse [s]			Impulse Bit [μN·s]			Thrust to Power ratio [μN/W]		
	Measured	Estimated	Error	Measured	Estimated	Error	Measured	Estimated	Error
LES-6[1]	300	304	1·3%	26	25·3	2·7%	14	13·7	2·1%
LES-8/9[1]	1,000	997	0·3%	297	284	4·4%	14·85	14·23	4·2%
Primex[11]	1,121	1,030	8·1%	737	795	7·9%	17·4	18·5	6·3%

Table 3
Measured and estimated parameters using the modified snowplow model

Thruster	Specific Impulse [s]			Impulse Bit [μN·s]			Thrust to Power ratio [μN/W]		
	Measured	Estimated	Error	Measured	Estimated	Error	Measured	Estimated	Error
LES-6[1]	300	119	60%	26	45	73%	14	24	71%
LES-8/9[1]	1,000	430	57%	297	163	45%	14·85	8·2	45%
Primex[11]	1,121	1,385	24%	737	526	29%	17·4	12·3	29%

The investigated wide range of thruster parameters and the good agreement between results of the modified model and the measured performance prove that the modified model is reliable and accurate enough to be used to simulate the performance of pulsed plasma thrusters having different energy level, capacitance, and geometries. Figure 5 illustrates the current waveforms for the above three thrusters as estimated by the modified model. It is clear that the current discharges in a decaying sin wave establishing the known current reversal problem. Also, it is clear that the discharge current peaks in the first few microseconds and that the complete discharge concludes in less than 10 microseconds. The peak current values are 6kA, 18·8kA, and 20·5kA in LES-6, LES8/9, and Primex thrusters, respectively.

The discharge voltage starts with the initial value on the capacitor, which is determined by the initial energy stored in the capacitor and its capacitance, as shown in Fig. 6. Also, the resulting thrust in one pulse is shown in Fig. 7, which indicates that the thrust diminishes in few micro seconds after it reaches a peak. It is clear from this Fig. that the current reversal phenomenon does not affect the thrust direction. This thrust variation may not be accepted by the satellite control system during one pulse. In fact these oscillations occur within the discharge time, which usually lies in the order of microsecond. Comparing this with spacecraft dynamics which reveals order of seconds or milliseconds, it is expected that the spacecraft will recognise this variation in thrust

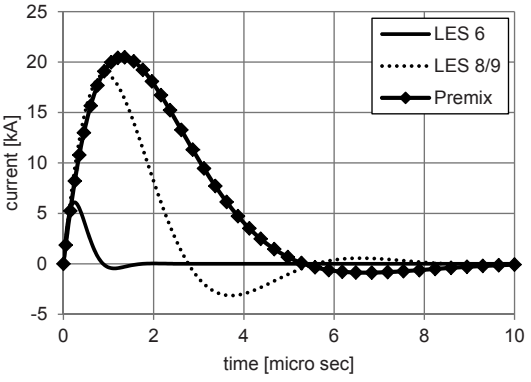


Figure 5. Current waveform for LES-6, LES 8/9, and Primex thrusters.

https://doi.org/10.1017/S0001924000008599 Published online by Cambridge University Press

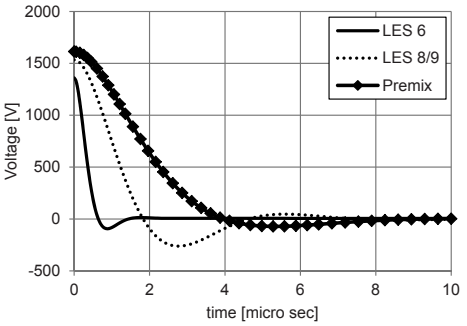


Figure 6. Voltage waveform for LES-6, LES 8/9, and Primex thrusters.

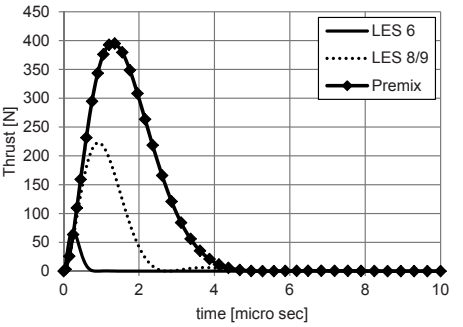


Figure 7. Thrust as function of time for LES-6, LES 8/9, and Primex thrusters.

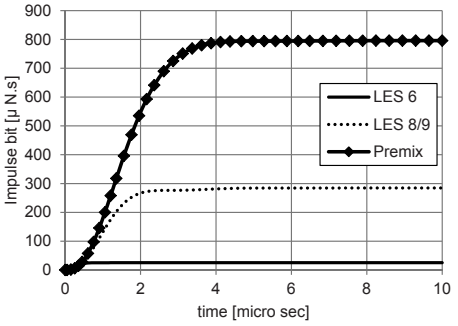


Figure 8. Development of impulse for LES-6, LES 8/9, and Primex thrusters.

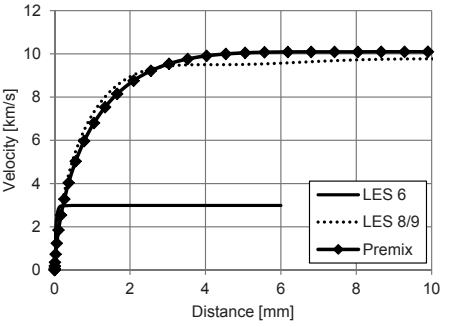


Figure 9. Plasma velocity along thruster channel for LES-6, LES 8/9, and Primex thrusters.

as one pulse with an average thrust value. The average thrust will be equal to the impulse bit, if a frequency of 1·0Hz is adopted. The development of impulse in one pulse is plotted in Fig. 8, which confirms the estimated values of impulse bit given in Table 2.

A frequency of about 1·0Hz is commonly used, thus, the power needed is equal to the initial energy of the capacitor. However, as shown in the previous Figure , the period of charge/discharge of the capacitor is in the order of tens of micro seconds. This permits the operation of PPT at lower energy but higher frequency rather than at a higher energy but lower frequency. This concept is called micro-pulsing operation, and it allows for reductions in the energy storage unit volume and mass without paying a penalty in thrust[12]. However, the lifetime of the capacitor, which is measured by number of charging/discharging cycles, should be estimated carefully, if micro-pulsing operation is considered.

This means that the operation at high frequency and low energy would reduce the power level and thus allows for smaller power to be supplied to the thruster. However, this would constrain the life time of the capacitor and hence the life time of the thruster. Normally, the thruster would work for large number of cycles during the space mission. If the required life time for the thruster is longer than that of the capacitor due to the micro-pulsing operation, the designer has to reduce the frequency and increase the energy. The developed model would be very helpful in evaluating the maximum allowable frequency for Micro-pulsing.

The pulsing rate of the pulsed plasma thruster determines the level of power absorbed from the satellite power subsystem. Thus, the same thruster can work at various power level using

https://doi.org/10.1017/S0001924000008599 Published online by Cambridge University Press

constant energy and variable pulse rate. Off course, increasing the pulse rate can result in steady state operation for the thruster and increases the total impulse for certain duration. Consequently, the thruster may be used for missions that require large velocity changes. On the other hand decreasing the pulse rate results in working at smaller power level while increasing the mission time and causes shot to shot variation (unsteady operation) with increased losses.

Finally, the plasma velocity along the thruster channel is plotted in Fig. 9. This Figure can be used to estimate the minimum thruster channel length for certain design. It is obvious from this Figure that lengths of about 0·5mm, 4·0mm, and 6·0mm are needed for LES-6, LES 8/9, and Primex thrusters, respectively. The plasma reaches its maximum speed at this distance and any additional length will add weight and size that are not needed. This can give valuable insight on the optimum electrode length. Thus, for fixed electric parameters, the electrode length can be reduced to avoid unnecessary losses without affecting the maximum velocity reached and hence without affecting impulse bit, average thrust, and specific impulse[13].

In the concept of system optimisation, many factors must be considered. These factors are thruster efficiency, specific impulse, and impulse bit. The efficiency and specific impulse are needed to be maximised, while the impulse bit must be minimised as possible if the thruster is to be employed in precision control missions. The thruster geometrical parameters and the circuit operating parameters can be changed to produce the optimum performance indices. A 33μF capacitor, and electrode gap, h = 2·5cm, are employed for all coming results. These values are adopted as average values from previous work[11], while the aspect ratio and energy will be changed. It was found that changing both electrode gap and width simultaneously, in a way such that the aspect ratio remains constant, doesn't affect the performance parameters. On the other hand, if the aspect ratio is altered, by changing electrode gap or width, the performance parameters would change. Thus, the electrode gap was kept constant, at 2·5cm, and the electrode width was varied. This electrode gap is reasonable for the igniter to be able to ablate propellant from the full propellant surface. The minimum investigated width was 0·63cm, which is close to the width of previously designed thrusters, such as EO-1 thruster[14].

Figure 10 shows contours of constant specific impulse if thruster aspect ratio, h/d, and initial energy in the capacitor are changed. It is obvious that to work at higher specific impulse, energy and/or aspect ratio has to be increased. The reduction in propellant mass gained by increasing the specific impulse should be weighed against the increase in size and mass of the capacitor, if energy is to be increased. On the other hand, increasing the aspect ratio is more promising, as it means a reduction in the electrode width for the same electrode gap.

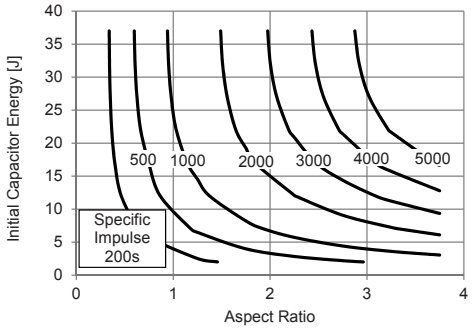


Figure 10. Initial capacitor energy as function of aspect ratio (contours of constant specific impulse) C = 33μF, and h = 2·5cm.

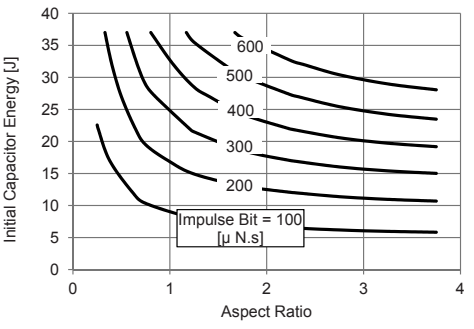


Figure 11. Initial capacitor energy as function of aspect ratio (contours of constant impulse bit) C = 33μF, and h = 2·5cm.

https://doi.org/10.1017/S0001924000008599 Published online by Cambridge University Press

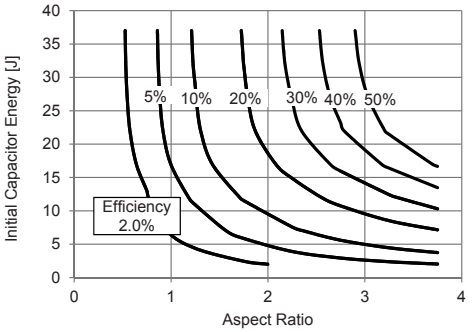


Figure 12. Initial capacitor energy as function of aspect ratio (contours of constant efficiency) C = 33μF, and h = 2·5cm.

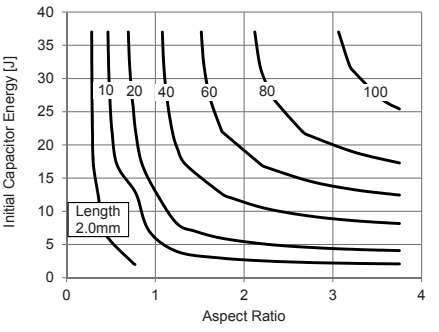


Figure 13. Initial capacitor energy as function of aspect ratio (contours of constant channel length) C = 33μF, and h = 2·5cm.

Figure 11 illustrates contours of constant impulse bit at different aspect ratio and energy. This Figure is generated by searching for the combinations of capacitor energy and aspect ratio that produce certain value of impulse bit. The higher impulse bit will be preferred for missions such as orbit insertion, while small impulse bit will be must if the thruster is to be used in a precision control mission. Therefore, thrusters used in orbit insertion missions will employ large aspect ratio and/or high energy, while thrusters used in precision control missions will utilise small aspect ratio and/or small energy. Working with small impulse bit will be accompanied with reduction in specific impulse. The effect of reduced specific impulse is to use larger amount of propellant mass. However, it is known that precision control missions don't require much velocity change and hence small amount of propellant would be enough to perform the mission even with the small specific impulse.

The main weak point of the pulsed plasma thruster is its low efficiency mainly due to the poor utilisation of ablated mass. Figure 12 displays contours of constant efficiency at different aspect ratio and energy. The efficiency is low if compared to that of other electric propulsion, and it can reach up to 50% at very high energy and/or very large aspect ratios. Finally, Fig. 13 demonstrates contours of constant minimum channel length calculated based on the distance at which the plasma reaches its maximum velocity. The increased channel length is apparent if a higher specific impulse and efficiency are required, and this will add weight and size to the thruster. The reduction in the required propellant mass due to the increase in specific impulse should be weighed against the added weight due to the increase in electrode length. Moreover, using large electrode length increases the electrode erosion especially for the anode.

Electrode erosion is generally much more severe at the anode than that at the cathode. Therefore, the anode, for some thrusters, is machined from a single piece of stainless steel to mitigate this effect[15]. If the anode erodes too quickly, the anode and therefore thruster lifetime will be significantly shorter than desired[16]. Erosion can become important if the specific impulse is too high, in which case the ablated mass can be insufficient to provide current carriers to the discharge. In a PPT with Isp > 3,000s, the discharge will seek charge carriers from the electrode and insulator material. Results for PPT, operating at very high specific impulse, must be viewed with caution (1). However, for flight-qualified PPTs, electrode and insulator erosion has not proven to be a life-limiting issue, principally because of the relatively large ablated mass[1].

However, Ref. 17 argues that the spacing between electrodes needs to be tuned in order to optimise the performance of the PPT. In a work on side fed PPT[17], it was shown that as the

https://doi.org/10.1017/S0001924000008599 Published online by Cambridge University Press

electrode spacing continues to increase beyond some optimal point, efficiency begins to decrease. No declaration is given for this drop in efficiency; however, it is probably due to the inability of the igniter to ablate the propellant from the area far away from the cathode, if large electrode spacing is used. The ablated mass from this far away area will be due to late ablation that occurs as a result of the high temperature of the plasma. This effect causes a reduction of the efficiency as this mass is accelerated by thermal effects only after lasting of the electric pulse. Ultimately, post pulse late-time ablation in these thrusters defines operation and performance capability by sustaining significant propellant mass loss per pulse that fails to contribute efficiently to thrust. This phenomenon is called late-time ablation and has been estimated to account for 40–90% of the total mass loss from various sources[18].

Also, due to the high temperature of the plasma, heat will be lost to thruster walls and surroundings, and this will decrease the overall efficiency of the thruster. According to a previous work done at University of Illinois[19], this heat loss is about 14% of the available energy. This effect is not accounted for in this model as well as the known snowplow model. However, for the preliminary design tasks, it would be good to have a simple model that gives indication about the dimensions and electrical parameters of the thruster to suit certain space mission.

Viscous layers and sheath interactions are particularly important for small dimensions, as viscous effects become important and there might be an overlap of electro-dynamic and gas dynamics scales[20]. At the largest considered aspect ratio, the electrode width is in the order of 0·62cm, which is still big if compared with the boundary-layer thickness, where viscous effects take place. Moreover, this effect is not considered in the original snowplow model, and this paper proposes a modified snowplow model that accounts for the variation of plasma resistance and ablated mass per pulse with thruster geometry and electrical parameters. However, it is believed that the effect of viscosity and sheath interactions will remain a weak point for the proposed model as well as the known snowplow model.

4.0 CONCLUSIONS

In this paper, the snowplow model of pulsed plasma thruster was modified by adding the effects of variation of plasma resistance, inductance, and ablated mass per pulse with energy and thruster geometry. A semi-empirical correlation was formulated for the ablated mass per unit area as function of capacitor energy. The above three parameters were added to the known snowplow model, and verifications for the modified model were made by comparing its results with experimental measurements for three known space qualified pulsed plasma thrusters. Good agreement between the model results and the given data of these thrusters has been proved. The maximum error is estimated to be about 8% when using the modified model. On the other hand, the conventional snowplow model produces error up to about 70%.

The modified model was then employed to optimise thruster performance by changing geometrical and electrical parameters. The specific impulse, efficiency and impulse bit can be increased by working at higher energy levels and/or employing large aspect ratio. The use of high energy will be accompanied with increase in the mass and size of the energy storage unit. The utilisation of large aspect ratio will be supplemented by increase in the late-time-ablation phenomenon if the gap between electrodes is increased, and this might cause a drop in the thruster efficiency. However, the aspect ratio can be increased by decreasing the electrode width while keeping the gap spacing constant at certain proper average value. The increase in specific impulse and thruster efficiency will be accompanied by increase in the required channel length, which might cause increase in the size and weight of the thruster, as well as the erosion rate of electrode material.

https://doi.org/10.1017/S0001924000008599 Published online by Cambridge University Press

Design charts for the main performance indices have been introduced to help the designer in selecting the proper thruster size and energy level for given mission requirements. These charts have not been produced before and they can give a good estimation for the geometrical and electrical parameters that would optimise the thruster performance for certain type of space missions.

REFERENCES

1. BURTON, R.L and TURCHI, P.J. Pulsed plasma thruster, *J Propulsion and Power*, September-October 1998, **14**, (5), pp 716-735.
2. JAHN, R.G. *Physics of Electric Propulsion*, Dover Publications Inc, 2006.
3. ZIEMER, J.K. Performance Scaling of Gas-Fed Pulsed Plasma Thrusters, PhD Thesis, Department of Mechanical and Aerospace Engineering, Princeton University, New Jersey, USA, June 2001.
4. ZIEMER, J.K. and CHOUEIRI, E.Y. Scaling laws for electromagnetic pulsed plasma thrusters, *Plasma Sources Science and Technology*, 2001, **10**, pp 395-405.
5. BURTON, R.L., WILSON, M.J. and BUSHMAN, S. Energy balance and efficiency of the pulsed plasma thruster, 34th AIAA/ASME/SAE/ASEE Joint Propulsion Conference and Exhibit, Cleveland, OH, USA, 13-15 July 1998.
6. LAPERRIER, D.D. Electromechanical modelling and open-Loop control of parallel-plate pulsed plasma micro thruster with applied magnetic fields, MSc Thesis, Worcester Polytechnic Institute, Worchester, UK, 2005.
7.. ECKMAN, R.F. Langmuir Probe Measurements in the Plume of a Pulsed Plasma Thruster, MSc thesis, Worcester Polytechnic Institute, Worchester, UK, 1999
8. IGARASHI, M. *et al* Performance improvement of pulsed plasma thruster for micro satellite, IEPC-01-152, 27th International Electric Propulsion Conference, Pasadena, California, USA, October, 2001.
9. MARQUES, R.I. A Mechanism to Accelerate the Late Ablation in Pulsed Plasma Thruster, PhD Thesis, University of Southampton, Southampton, UK, 2009.
10. SCHÖNHERR, T., NAWAZ, A., HERDRICH, G., RÖSER, H-P and AUWETER-KURTZ, M. Influence of electrode shape on performance of pulsed magnetoplasmadynamic thruster SIMP-LEX, *J Propulsion and Power*, March–April 2009, **25**, (2), pp 380-386.
11. ARRINGTON, L., HAAG, T. PENCIL, E. and MECKEL, N. A performance comparison of pulsed plasma thruster electrode configurations, NASA-TM 97-206305, also IEPC-97-127, 25th International Electric Propulsion Conference, Cleveland, Ohio, USA, August 1997.
12. ARRINGTON, L. Evaluation of pulsed plasma thruster micropulsing, NASA/CR–2004-213209, also, AIAA–2004–3458, 40th AIAA/ASME/SAE/ASEE Joint Propulsion Conference and Exhibit, Florida, USA, July 2004.
13. NAWAZ, A. and LAU, M. Plasma sheet velocity measurement techniques for the pulsed plasma thruster SIMP-LEX, IEPC-2011-248, the 32nd International Electric Propulsion Conference, Wiesbaden, Germany, September 2011.
14. GATSONIS, N., ZWAHLEN, J., WHEELOCK, A., PENCIL, E. and KAMHAWI, H. Pulsed plasma thruster plume investigation using a current-mode quadruple probe method, *J Propulsion and Power,* March–April 2004, **20**, (2), pp 243-254.
15. RAYBURN, C.D., CAMPBELL, M.E. and MATTICK A.T. Pulsed plasma thruster system for microsatellites, *J Spacecraft and Rockets*, January–February 2005, **42**, (1), pp 161-170.
16. LAYSTROM, J.K., BURTON, R.L. and BENAVIDES G.F. Geometric optimization of a coaxial pulsed plasma thruster, AIAA 2003-5025, 39th AIAA/ASME/SAE/ASEE Joint Propulsion Conference and Exhibit, July 2003.
17. RAYBURN, C., CAMPBELL, M., HOSKINS, W.A. and CASSADY R.J. Development of a micro pulsed plasma thruster for the Dawgstar nanosatellite, AIAA-2000-3256.
18. ANTONSEN, E.L., BURTON, R.L., REED, G.A. and SPANJERS G.G. Effects of postpulse surface temperature on micropulsed plasma thruster operation, *J Propulsion and Power*, September–October 2005, **21**, (5), pp 877-883.
19. RYSANEK, F. and BURTON, R. Performance and heat loss of a coaxial Teflon pulsed plasma thruster, IEPC-01-151, the 27th International Electric Propulsion Conference, Pasadena, California, USA, 15-19 October 2001.
20. LIN, G. AND KARNIADAKIS, G.E. A high-order discontinuous Galerkin method for modelling micro-pulsed plasma thrusters, IEPC-01-154, the 27th International Electric Propulsion Conference, Pasadena, California, USA, 15-19 October, 2001.

https://doi.org/10.1017/S0001924000008599 Published online by Cambridge University Press